Oon, CS, Amiri, A, Chew, BT, Kazi, SN, Shaw, A and Al-Shamma'a, A

Increase in Convective Heat Transfer over A Backward-Facing Step Immersed in A Water-Based Tio2 Nanofluid

Article

Citation (please note it is advisable to refer to the publisher's version if you intend to cite from this work)

Oon, CS, Amiri, A, Chew, BT, Kazi, SN, Shaw, A and Al-Shamma'a, A (2018) Increase in Convective Heat Transfer over A Backward-Facing Step Immersed in A Water-Based Tio2 Nanofluid. Heat Transfer Research, 49 (15). pp. 1419-1429. ISSN 1064-2285

Convective heat transfer growth over a backward-facing step using water-based TiO_2 nanofluid

C.S. Oon,[1, 2,] * Ahmad Amiri,[3,]* B.T. Chew,[1] S.N. Kazi,[1] A. Shaw,[2] & A. Al-Shamma'a[2]

[1]Department of Mechanical Engineering, Faculty of Engineering, University of Malaya, 50603 Kuala Lumpur, Malaysia

[2]School of Built Environment, Liverpool John Moores University, Byrom Street, Liverpool, L3 3AF, United Kingdom

[3]Department of Chemical Engineering, Faculty of Engineering, Ferdowsi University of Mashhad, Mashhad, Iran

*Address all correspondence to: Ahmad Amiri, Department of Chemical Engineering, Faculty of Engineering, Ferdowsi University of Mashhad, Mashhad, Iran, E-mail: ahm.amiri@gmail.com; or C.S. Oon, Department of Mechanical Engineering, Faculty of Engineering, University of Malaya, 50603 Kuala Lumpur, Malaysia, E-mail: oonsean2280@yahoo.com

ABSTRACT: Investigation of flow separation and reattachment of 0.2% water-based TiO_2 nanofluid in an annular sudden expansion is presented in this paper. Such flows occur in various engineering and heat transfer applications. Computational fluid dynamics package (FLUENT) is used to study turbulent nanofluid flow in this research. Only a quarter of the annular pipe is developed and simulated as it has symmetrical geometry. Standard k-epsilon second order implicit, pressure based-solver equations are applied. Reynolds numbers between 17050 and 44545, step height ratio of 1.82 and constant heat flux of 49050 W/m^2 were utilized in the simulation. Numerical simulation results show that with the increase of Reynolds number increases the heat transfer coefficient and the Nusselt number. Moreover, the surface temperature dropped to its lowest value after the expansion and then gradually increased along the pipe.

Finally, the chaotic movement and high thermal conductivity of the TiO_2 nanoparticles have contributed to the overall heat transfer enhancement of the nanofluid.

KEY WORDS: heat transfer, computational fluid dynamics, TiO_2, nanofluid

Nomenclature

Cp	Heat capacity, J/kg K
D	Diameter, m
H_x	Heat transfer coefficient, W/m^2 K
K	Thermal conductivity, W/m K
Nu	Nusselt number
q	Heat flux, W/m^2
Re	Reynolds number
T	Temperature, °C
U	Velocity, m/s
x	local distance, m
D_h	Hydraulic diameter, m
TiO_2	Titanium dioxide
L	Length, m

Greek symbols

ϕ	Volume fraction
ρ	Density, kg/m^3
μ	Viscosity, Pa s
β	Ratio of the nanolayerthickness to the original particles radius

Subscripts

bf	Basefluid
nf	Nanofluid
p	Particles
f	Fluid
c	Convection
s	Surface
b	Bulk

1. INTRODUCTION

Flow separation at a boundary surface happens when the flow stream lines (the closest stream line to the boundary surface) break or separate away from the boundary surface and then the flow reattached. If the boundary surface is a finite dimension, then flow separation is expected due to the flow divergence over the downstream edge and the fluid flows away from the surface (Chang, 1976). Large amount of the research on separation flow were performed on circular pipe and rectangular duct flow however little is studied about heat transfer and flow phenomena in an annular passage. Such information is crucial for improving the performance of parallel and counter flow heat exchangers.

Also, the flow behind the backward-facing step is complex and includes different instability mechanisms, which the phenomenon after the step is illustrated in the Fig. 1 (Driver et al., 1987). An experimental have been conducted by Armaly et al. (1983) for an expansion ratio at 2 and downstream aspect ratio at 18. They concluded that a secondary recirculation region appears at the channel upper wall and the difference in primary recirculation zone length should be happened due to the secondary recirculation region destroying the two-dimensional character of the flow for Reynolds numbers more than 400 (Armaly et al., 1983). In addition, they reported that the behaviour of three-dimensional flow is transitional at the Reynolds range of 1200-6600.

Kaiktsis et al.(1996) studied two-dimensional simulations of flow for Reynolds numbers at 2500 and expansion ratio at 2. They illustrated that all asymptotic flow states are steady in the abovementioned range of Reynolds numbers. The effect of the step expansion ratio on the reattachment length of laminar flow for Reynolds range of 33-600 was investigated by Thangam and Knight (1989). It was observed that the non-dimensional reattachment length increases with expansion ratio. Also, the dependence of reattachment length on expansion ratio showed the opposite behaviour for the turbulent regime (Ötügen, 1991). According to the review of the literature in the turbulent regime over a step, Eaton and Johnston (1981) showed five parameters that can influence the flow structure: (i) initial boundary layer state, (ii) initial boundary layer thickness, (iii) freestream turbulence level, (iv) pressure gradient and (v) aspect ratio of the channel. But, a majority of reported studies was focused on the flow structure, while the interpretation of the heat transfer expansion, in particular in turbulent regime, can be much more difficult. Thus, the purpose of the present research is to compute the heat transfer rate to turbulent nanofluid flow in annular pipe and also to investigate the effect of flow separation due to sudden enlargement.

On the other hand, the mixture of different small particles in the basefluids have been used as a method to enhance the rate of heat transfer in various heat transfer instruments (Oon, Togun et al., 2012; Amiri et al., 2016). One of the reasons is the thermal conductivity of metal and carbon nanostructures exhibiting much higher thermal conductivity than those of the basefluids. Recently, nanofluids (mixing of nano sized particle with basefluid) have been widely studied and caught the attention of many researches (Shanbedi et al., 2014; Zubir et al., 2015; Amiri et al., 2016). This is due to their promising properties like high thermal conductivity, stable and poor tendency to clog in microchannels.

Numerous researchers have studied the effect of different nanoparticles on the heat transfer performance of heat transfer equipment. Different nanoparticles such as copper oxide (CuO), aluminum oxide (Al_2O_3), titanium dioxide (TiO_2), etc. have been used to produce nanofluids for heat transfer enhancement (Choi and Eastman 1995; Sohel et al., 2014). Lee et al. (1999) experimentally investigated the thermal conductivity of alumina/water, alumina/ethylene glycol and CuO/ethylene glycol. About 23% enhancement in the thermal conductivity of ethylene glycol was obtained by the researchers in the presence of CuO nanoparticles. Murshed et al. (2005) did a research in the thermal conductivity of TiO_2/water nanofluids. According to the results, there is a strong nonlinear correlation between the thermal conductivity and volume concentration of nanofluids.

Some metallic oxide nanoparticles TiO_2, CuO, etc have attracted many researchers in the field of heat transfer, because of their higher thermal conductivity and good dispersivity in different basefluids such as ethylene glycol, water and oils. The introduction of metal oxide nanoparticles into the common basefluids demonstrates a considerable enhancement in the heat transfer rate of these fluids due to increase in the interactions and collisions between the particle and basefluids (Dong et al., 2012; Jani et al., 2014). Heris et al. (2006) studied the convective heat transfer coefficient of Al_2O_3/water, Cu/water, and CuO/water nanofluids in a circular tube at constant wall-temperature condition and at laminar flow regime. The results showed that the convective heat transfer coefficient increased with the increase of Peclet number and nanoparticle concentration in the basefluid. Farajollahi et al. (2010) obtained the optimal concentration for TiO_2/water and Al_2O_3/water nanofluids. Nguyen et al. (2008) investigated the heat transfer performance of Al_2O_3/water nanofluids of different particle sizes and reported that as the size of nanoparticles increased, the heat transfer rates decreased.

On the other hand, some studies confirmed that nanoparticles with low particle concentration can considerably enhance the thermal conductivity of basefluids (Kwark, 2010). Among different metal oxide nanoparticles, titanium dioxide is selected as a promising and safe nanoparticle for human and is widely utilized for various issues such as biological, nanocomposite, and physical applications (Jayaseelan et al., 2013; Ohto et al., 2014). By looking at chemical activity, TiO_2 can be used to prepare a brilliant physical and chemical stability in different basefluids without any surfactant as stabilizer, which is the main source for reducing extra problems in the thermal equipment. So, TiO_2 with an appropriate dispersion can be a good subject to investigate.

2. METHODOLOGY

2.1. Design

In order to investigate the rate of heat transfer of water-based TiO_2 nanofluid in an asymmetric abrupt expansion computational fluid dynamic software (FLUENT) is chosen and utilized (Abu-Nada, 2008). Figure 2 shows the length of the annular pipe 1300mm with an inner diameter of 20mm. The red line along the outer pipe in the figure indicates the surface area heated at heat flux, q of 49050 W/m^2. The step heights were created by changing the diameter of the entrance tube (d) to 33mm, which is equivalent to the step height ratios of 1.82.

2.2. CFD Simulations

The heat transfer and flow behaviour through sudden expansion in an annular pipe can be investigated using numerical simulation (Yu and Choi, 2003). Figure 3 illustrates the geometry meshed utilizing the FLUENT software. The meshing results include the statistic nodes of 43383 and 74891 elements. Only a quarter of the annular pipe is drawn and simulated due to its symmetrical geometry.

Iterations were performed until their residual values dropped below $1 \cdot 10^{-4}$. Four distinct Reynolds numbers of 17050, 30720, 39992 and 44545 were selected to investigate in the simulation. All these Reynolds numbers fall in the fully developed turbulent flow region. The boundary condition for the inlet is set as velocity inlet. Both of the momentum and turbulent dissipation rate were set to second order upwind. Table 1 shows the computational conditions of the numerical simulation. Standard k-epsilon second order implicit, pressure based-solver equation is applied. The simulated fluid flow is treated as single phase flow rather that multiphase flow, the thermal physical properties of the nanofluid is important in this study. Thermophoresis effect is neglected in this study.

2.3. Data Processing

To investigate the influence of the TiO_2 on the thermal properties of pure water, the heat transfer coefficient (H_x) have been considered. The local heat transfer coefficient (H_x) is calculated by using Eq. (1).

$$H_x = q_c / (T_{sx} - T_{bx}) \tag{1}$$

where q_c convective heat flux, T_{sx} surface temperature and T_{bx} local bulk air temperature. Reynolds number can be calculated utilizing the Eq. (2):

$$Re_d = \rho_f \cdot U \cdot D_h / \mu_f \tag{2}$$

where ρ_f density of fluid, U velocity of fluid, D_h hydraulic diameter of the annular pipe and μ_f dynamic viscosity of the bulk fluid. The local Nusselt number (Nu) can be evaluated using Eq. (3):

$$Nu = H_x \cdot d / K_f \tag{3}$$

Where d is the diameter of pipe and K_f is the thermal conductivity of the bulk fluid.

Table 2 shows the thermal and physical properties of TiO_2 nanoparticles and water (Abu-

Nada, 2008). The nanoparticles are capable of increasing the thermal conductivity of the basefluids.

Thermal and physical properties of nanofluids such as thermal conductivity, specific heat, density and viscocity of nanofluids can be obtained by several suggested correlations (Pak and Cho 1998; Yu and Choi 2003; Drew and Passman 2006; Oon et al., 2014). The thermal conductivity of water-based TiO_2 nanofluids can be calculated by using Eq. (4):

$$K_{nf} = [(K_p + 2K_{bf} + 2\phi\,(K_p - K_{bf})(1+\beta)^3)\,/(K_p + 2K_{bf} - \phi\,(K_p - K_{bf})(1+\beta)^3)] \cdot K_{bf} \qquad (4)$$

where is the Knf is the thermal conductivity of nanofluid, Kp is the thermal conductivity of nanoparticles, Kbf thermal conductivity of basefluids and β ratio of the nanolayer thickness to the original particle radius. Generally, the value of $\beta = 0.1$, is selected in the calculation of the thermal conductivity of nanofluids. Equation (5) is utilized to calculate the density of nanofluids:

$$\rho_{nf} = \phi\rho_p + (1 - \phi)\,\rho_{bf} \qquad (5)$$

where ϕ volume fraction of the nanoparticles, ρ_{bf} density of basefluid and ρ_p density of nanoparticles. Equation (6) is used to calculate the heat capacity of nanofluids:

$$Cp_{nf} = \phi Cp_p + (1 - \phi)\,Cp_{bf} \qquad (6)$$

where Cp_{nf} heat capacity of nanofluids, Cp_{bf} heat capacity of basefluids and Cp_p heat capacity of nanoparticles. The viscosity of nanofluids is calculated by using Eq. (7) and only appropriate for the volume fraction less than 5.0 vol.%.

$$\mu_{nf} = (1 + 1.25\phi)\,\mu_{bf} \qquad (7)$$

where μ_{nf} viscosity of nanofluids and μ_{bf} viscosity of basefluids.

3. Results and Discussion

The graph of temperature versus distance for water-based TiO_2 nanofluid and water were illustrated in Fig. 4. The numerical simulation was conducted at 1.82 step height ratio and

Reynolds number of 39992. Temperature curves of the water and TiO_2 shown that there is a considerable drop in overall temperature as water-based TiO_2 nanofluid is utilized. This phenomena can be explained by the increase in thermal physical properties and chaotic movement of TiO_2 nanoparticles in the fluid.

Figure 5 shows the graph of heat transfer coefficient versus distance for water-based TiO_2 nanofluid and water. The results show sharp increment in heat transfer coefficient shortly after expansion and reduce gradually afterward. The overall heat transfer coefficient of the water-based TiO_2 nanofluid is higher than the water.

The graph of Nusselt number versus distance for water-based TiO_2 nanofluid and water is shown in Fig. 6. The curves of the heat transfer coefficient and Nusselt number show similar trend. Water-based TiO_2 nanofluid is observed to have higher Nusselt number compared to water, it can be due to the higher thermal conductivity of TiO_2 in nanofluid. The maximum Nusselt number is obtained shortly after the expansion, that maximum point is also known as the flow reattachment point where to separated stream reattached and maximize the heat transfer. The overall Nusselt number of water-based TiO_2 nanofluid is greater than the water.

The graph of surface temperature at the step height ratio of 1.82 with different Reynolds numbers are illustrated in Fig. 7. The results show a sudden decrease in temperature just after the expansion, which follows by a gradual increase along the tube. The flow reattachment occurs at the lowest temperature obtained along the pipe. The highest overall surface temperature is observed at Reynolds number of 17050 but decreases as the Reynolds number increases.

Figure 8 shows the local heat transfer coefficient versus the distance of water under the same conditions. A sudden growth in the heat transfer coefficient is obvious shortly after expansion and when Reynolds numbers increases the overall heat transfer coefficient is also increased.

The graph of the Nusselt numbers versus distance for water at different Reynolds numbers were shown in Fig. 9. The Nusselt number and the heat transfer coefficient illustrate similar trend in this case. The increase in Reynolds number have contributed to the higher overall Nusselt number.

4. CONCLUSIONS

In summary, increase in step height ratio and Reynolds number results in an increase in the heat transfer coefficient and Nusselt number. The surface temperature will drop to its lowest value after the expansion and then gradually increase along the pipe. Moreover, the minimum point of the surface temperature indicates the flow recirculation zone or reattachment point. The results also illustrate that the water-based TiO_2 nanofluids provides higher heat transfer performance compared to the water. Water-based TiO_2 nanofluids also present higher extent of the heat transfer coefficient and Nusselt number at the same condition such as step height ratio and Reynolds number. Finally, the chaotic movement and higher thermal conductivity of the TiO_2 nanoparticles have contributed to the overall heat transfer enhancement of the nanofluid compare to the water.

ACKNOWLEDGMENTS

The authors gratefully acknowledge Research Grant UMRG RP045C-17AET and PPP grant PG104-2016A, Faculty of Engineering, University of Malaya, Malaysia for support to conduct this research work. Special appreciations are also credited to Yew Sin Nee for her assistance and support in this research.

REFERENCES

Abu-Nada, E., Application of Nanofluids for Heat Transfer Enhancement of Separated Flows Encountered in a Backward Facing Step, *Int. J. Heat and Fluid Flow*, vol. **29**, no. 1, pp. 242–249, 2008.

Amiri, A., Arzani H. K., Kazi S., Chew B., and Badarudin A., Backward-Facing Step Heat Transfer of the Turbulent Regime for Functionalized Graphene Nanoplatelets Based Water–Ethylene Glycol Nanofluids, *Int. J. Heat and Mass Trans.*, vol. **97**, pp. 538–546, 2016.

Amiri, A., Shanbedi M., Chew B., Kazi S., and Solangi K., Toward Improved Engine Performance with Crumpled Nitrogen-Doped Graphene Based Water–Ethylene Glycol Coolant, *Chem. Eng. J.*, vol. **289**, pp. 583–595, 2016.

Armaly, B. F., Durst F., Pereira J., and Schönung B., Experimental and Theoretical Investigation of Backward-Facing Step Flow, *J. Fluid Mech.*, vol. **127**, pp. 473–496, 1983.

Chang, P., Control of Flow Separation: Energy Conservation, Operational Efficiency, and Safety, *NASA STI/Recon Tech. Rep. A*, vol. **77**, p. 11232, 1976.

Choi, S. U. S. and Eastman, J. A., Enhancing Thermal Conductivity of Fluids with Nanoparticles, *Proc. of the 1995 ASME Int. Mech. Eng. Cong. and Exp.*, vol. **231**, 1995, Pages 99–105, 1995.

Dong, S., Zheng L., Zhang X., and Zhang J., Heat Transfer Enhancement in Microchannels by Utilizing the Al_2O_3−Water Nanofluid, *Heat Trans. Res.*, vol. **43**(8). pp. 695–707, 2012.

Drew, D.A. and Passman S. L., Theory of Multicomponent Fluids, *Springer Science & Business Media*, 2006.

Driver, D.M., Seegmiller H. L., and Marvin J. G., Time-Dependent Behavior of a Reattaching Shear Layer, *AIAA J.*, vol. **25**, no. 7, pp. 914–919, 1987.

Eaton, J. and Johnston J., A Review of Research on Subsonic Turbulent Flow Reattachment, *AIAA J.*, vol. **19**, no. 9, pp. 1093–1100, 1981.

Farajollahi, B., Etemad S. G. and Hojjat M., Heat Transfer of Nanofluids in a Shell and Tube Heat Exchanger, *Int. J. Heat and Mass Trans.*, vol. **53**, no. 1, pp. 12–17, 2010.

Heris, S.Z., Etemad S.G., and Esfahany M.N., Experimental Investigation of Oxide Nanofluids

Laminar Flow Convective Heat Transfer, *Int. Commun. in Heat and Mass Trans.*, vol. **33**, no. 4, pp. 529–535, 2006.

Jani, S., Mahmoodi M., Amini M., and Akbari M., Free Convection in Rectangular Enclosures Containing Nanofluid with Nanoparticles of Various Diameters, *Heat Trans. Res.*, vol. **45**, no. 2, pp. 145–169, 2014.

Jayaseelan, C., Rahuman A. A., Roopan S. M., Kirthi A. V., Venkatesan J., Kim S. K., Iyappan M., and Siva C., Biological Approach to Synthesize Tio_2 Nanoparticles using Aeromonas Hydrophila and Its Antibacterial Activity, *Spectrochimica Acta Part A: Mol. and Biomol. Spectroscopy*, vol. **107**, pp. 82–89, 2013.

Kaiktsis, L., Karniadakis G. E., and Orszag S. A., Unsteadiness and Convective Instabilities in Two-Dimensional Flow over a Backward-Facing Step, *J. Fluid Mech.*, vol. **321**, pp. 157–187, 1996.

Kwark, S. M., Kumar R., Moreno G., Yoo J., and You S. M., Pool Boiling Characteristics of Low Concentration Nanofluids, *Int. J. of Heat and Mass Trans.*, vol. **53**, no. 5, pp. 972–981, 2010.

Lee, S., Choi S. S., Li S., and Eastman J., Measuring Thermal Conductivity of Fluids Containing Oxide Nanoparticles, *J. Heat Trans.*, vol. **121**, no. 2, pp. 280–289, 1999.

Murshed, S., Leong K., and Yang C., Enhanced Thermal Conductivity of Tio_2-Water Based Nanofluids, *Int. J. Therm. Sci.*, vol. **44**, no. 4, pp. 367–373, 2005.

Nguyen, C., Desgranges F., Galanis N., Roy G., Maré T., Boucher S., and Mintsa H.A., Viscosity Data for Al_2O_3–Water Nanofluid—Hysteresis: Is Heat Transfer Enhancement using Nanofluids Reliable? *Int. J. Therm. Sci.*, vol. 47(2), pp. 103-111, 2008.

Ohto, T., Mishra A., Yoshimune S., Nakamura H., Bonn M., and Nagata Y., Influence of Surface Polarity on Water Dynamics at the Water/Rutile Tio_2 (110) Interface, *J. Phys.: Condensed Matter*, vol. **26**, no. 24, p. 244102, 2014.

Oon, C., Al-Shamma'a A., Kazi S., Chew B., Badarudin A., and Sadeghinezhad E., Simulation of Heat Transfer to Separation Air Flow in a Concentric Pipe, *Int. Commun. in Heat and Mass Trans.*, vol. **57**, pp. 48–52, 2014.

Oon, C., Togun H., Kazi S., Badarudin A., Zubir M., and Sadeghinezhad E., Numerical Simulation of Heat Transfer to Separation Air Flow in an Annular Pipe, *Int. Commun. in Heat and Mass Trans.*, vol. **39**, no. 8, pp. 1176–1180, 2012.

Ötügen, M., Expansion Ratio Effects on the Separated Shear Layer and Reattachment Downstream of a Backward-Facing Step, *Exp. in Fluids*, vol. **10**, no. 5, pp. 273–280, 1991.

Pak, B.C. and Cho Y.I., Hydrodynamic and Heat Transfer Study of Dispersed Fluids with Submicron Metallic Oxide Particles, *Exp. Heat Trans. Int. J.*, vol. **11**, no. 2, pp. 151–170, 1998.

Shanbedi, M., Heris S.Z., Amiri A., Adyani S., Alizadeh M. and Baniadam M., Optimization of the Thermal Efficiency of a Two-Phase Closed Thermosyphon using Active Learning on the Human Algorithm Interaction, *Num. Heat Trans., Part A: Appl.*, vol. **66**, no. 8, pp. 947–962, 2014.

Sohel, M., Khaleduzzaman S., Saidur R., Hepbasli A., Sabri M.and Mahbubul I., An Experimental Investigation of Heat Transfer Enhancement of a Minichannel Heat Sink using Al_2O_3–H_2O Nanofluid, *Int. J. Heat and Mass Trans.*, vol. **74**, pp. 164–172, 2014.

Thangam, S. and Knight D.D., Effect of Stepheight on the Separated Flow Past a Backward Facing Step, *Phys. of Fluids A*, vol. **1**, pp. 604–606, 1989.

Yu, W. and Choi S., The Role of Interfacial Layers in the Enhanced Thermal Conductivity of Nanofluids: A Renovated Maxwell Model, *J. Nanopart. Res.*, vol. **5**, nos. 1-2, pp. 167–171, 2003.

Zubir, M.N.M., Badarudin A., Kazi S., Misran M., Amiri A., Sadri R. and Khalid S., Experimental Investigation on the Use of Highly Charged Nanoparticles to Improve the Stability of Weakly

Charged Colloidal System, *J. Colloid and Inter. Sci.*, vol. **454**, pp. 245–255, 2015.

TABLE 1: Computational conditions of the numerical simulations

Computational conditions	
Density	1000 kg/m^3
Viscosity	$1.7894 \cdot 10^{-5}$ Kg/m·s
Space/Time	2D/unsteady, second order implicit
Residual error	$1 \cdot 10^{-4}$
Pressure	101 325 Pa
Inlet boundary type	Velocity inlet
Outlet boundary type	Pressure outlet
Viscous model	k & ε
Interpolating Scheme (turbulence & momentum)	Second-order upwind

TABLE 2: Thermal physical properties of TiO_2 nanoparticles

Property	**TiO_2 nanoparticles**	**Water as the base fluid**	**TiO_2 nanofluid (0.2%)**
Density (kg/m^3)	4250	998.2	1004.7
Cp (heat capacity, J/kg K)	686.2	4182	4175
Thermal conductivity (W/m.K)	8.9538	0.6	0.6208

FIG. 1: Flow separation and reattachment in a sudden expansion pipe

FIG. 2: Schematic diagram of flow in an annular pipe with sudden expansion

FIG. 3: Meshing of the geometry

FIG. 4: Graph of temperature versus distance for TiO_2 nanofluid and water

FIG. 5: Graph of heat transfer coefficient versus distance for TiO_2 nanofluid and water

FIG. 6: Graph of Nusselt number versus distance for TiO_2 nanofluid and water

FIG. 7: Graphical representation of temperature variation with distance for TiO_2 nanofluid at different Reynolds numbers

FIG. 8: Graphical representation of heat transfer coefficient variation with distance for TiO_2 nanofluid at different Reynolds numbers

FIG. 9: Graphical representation of Nusselt number variation with distance for TiO_2 nanofluid at different Reynolds numbers

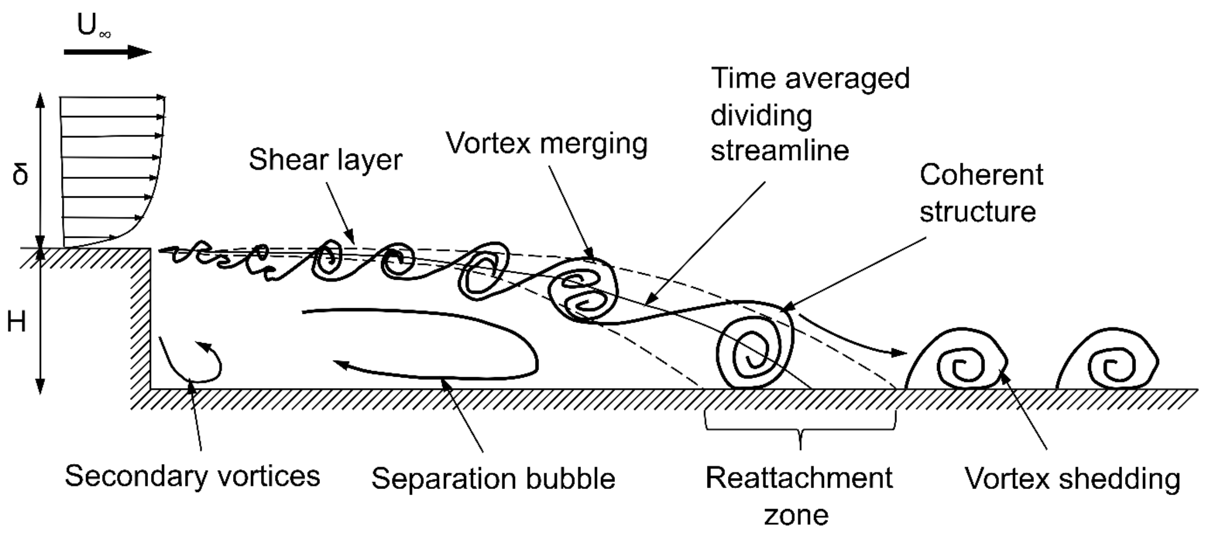

U_∞
δ
H
Shear layer
Vortex merging
Time averaged dividing streamline
Coherent structure
Secondary vortices
Separation bubble
Reattachment zone
Vortex shedding

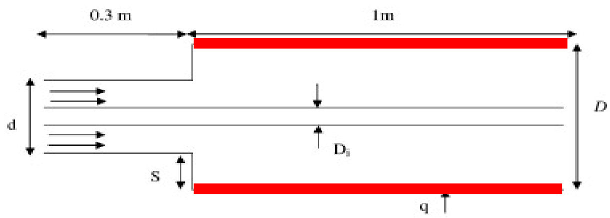

0.3 m
1m
d
D
D_j
S
q

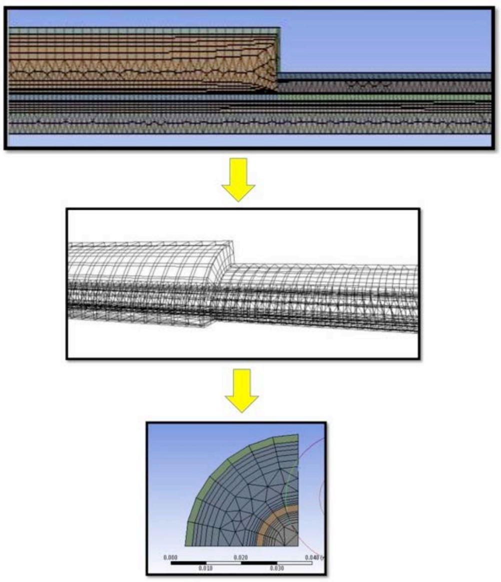
0.000
0.020
0.040
0.010
0.030

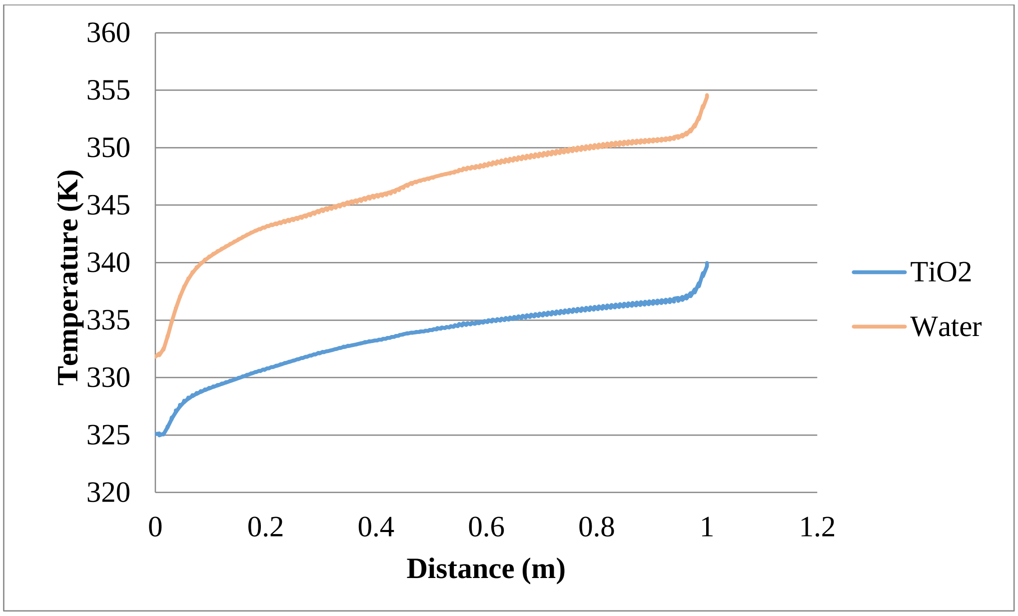

360
355
350
345
340
335
330
325
320
Temperature (K)
0
0.2
0.4
0.6
0.8
1
1.2
Distance (m)
TiO2
Water

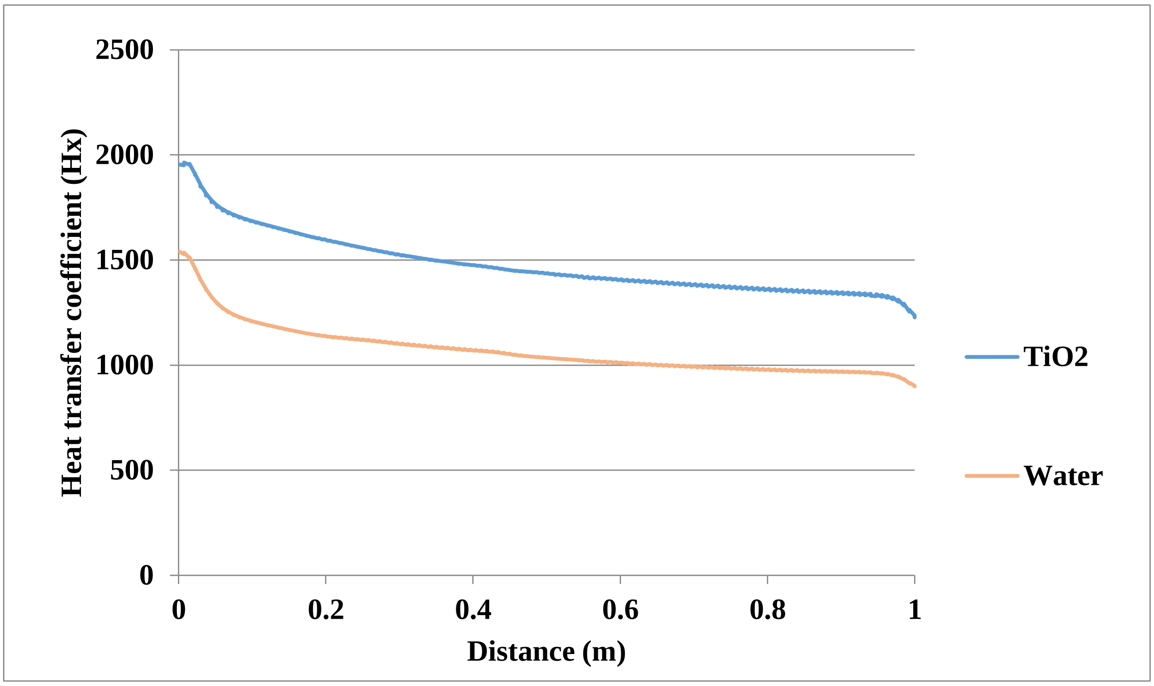

2500
2000
1500
1000
500
0
Heat transfer coefficient (Hx)
0
0.2
0.4
0.6
0.8
1
Distance (m)
TiO2
Water

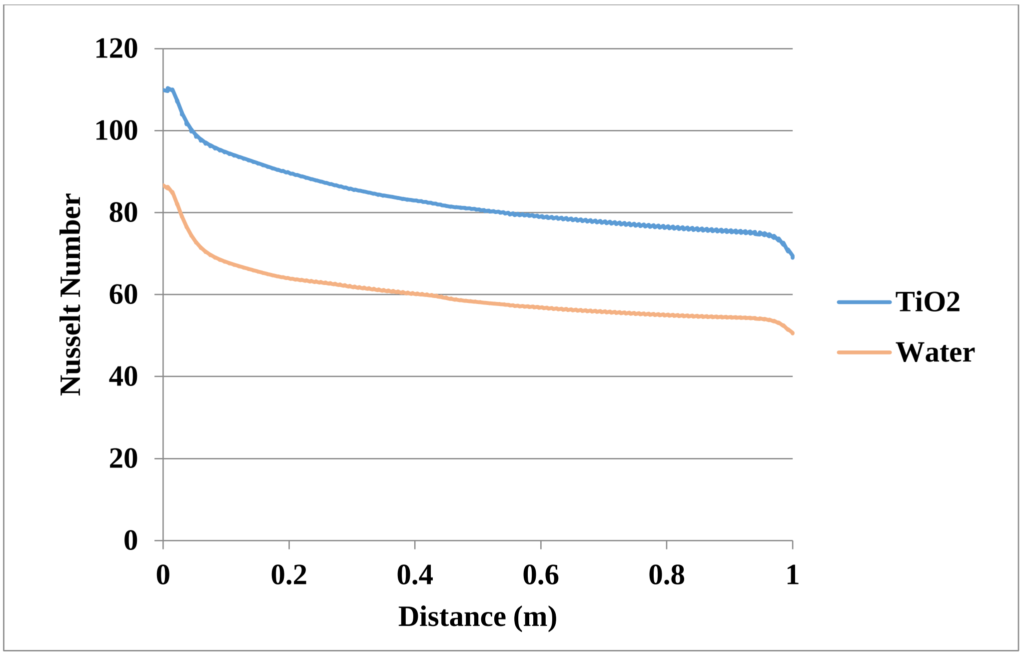
120
100
80
60
40
20
0
Nusselt Number
0
0.2
0.4
0.6
0.8
1
Distance (m)
TiO2
Water

.

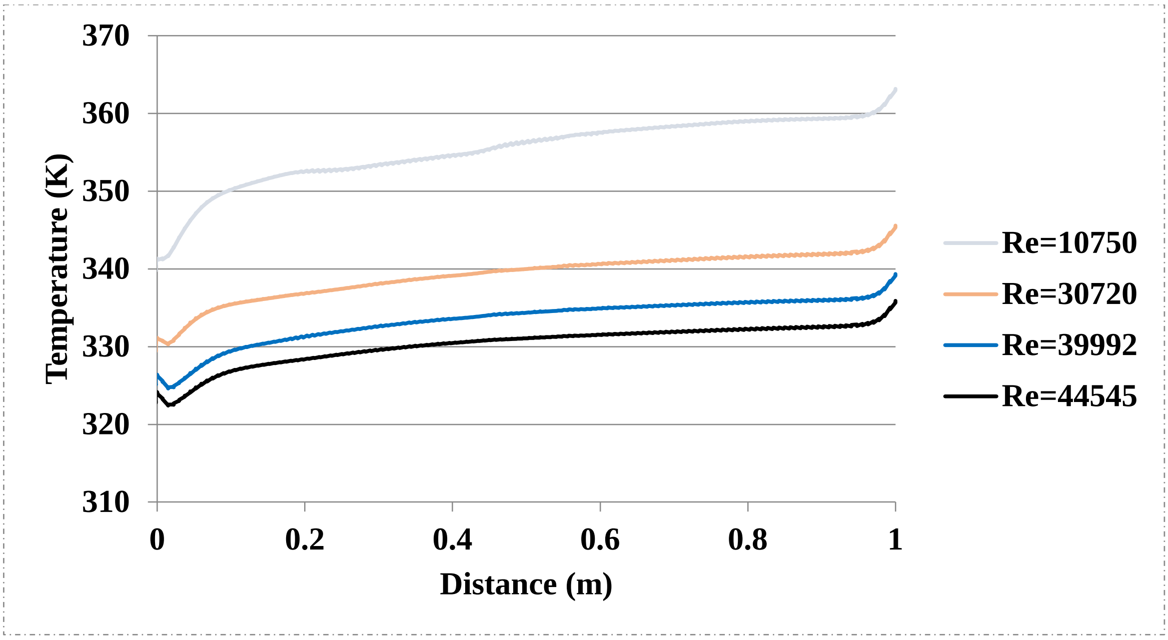

370
360
350
340
330
320
310
Temperature (K)
0
0.2
0.4
0.6
0.8
1
Distance (m)
Re=10750
Re=30720
Re=39992
Re=44545

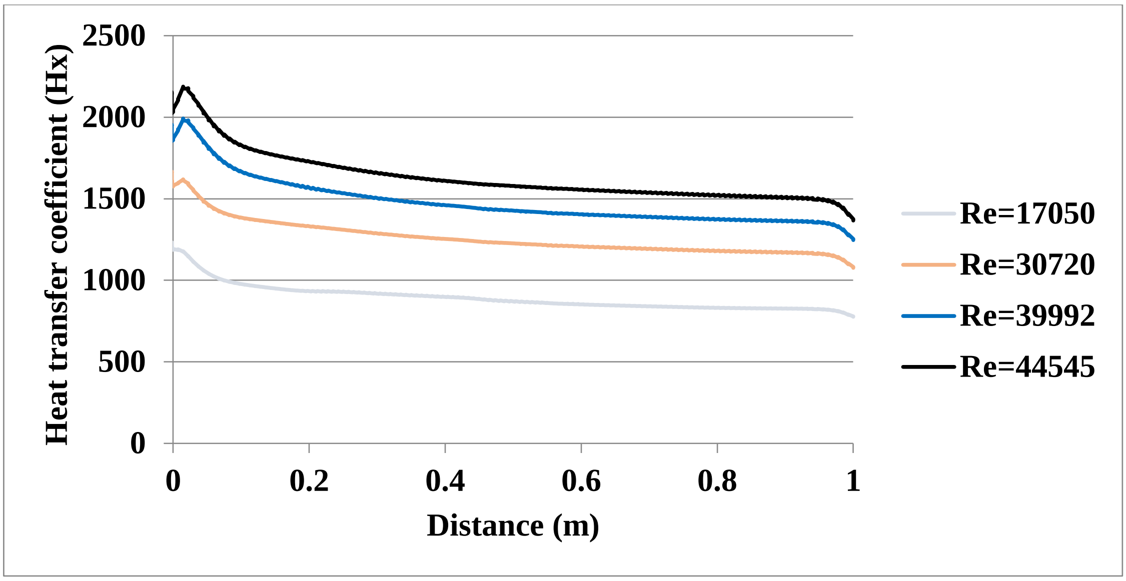

Heat transfer coefficient (Hx)
2500
2000
1500
1000
500
0
0
0.2
0.4
0.6
0.8
1
Distance (m)
Re=17050
Re=30720
Re=39992
Re=44545

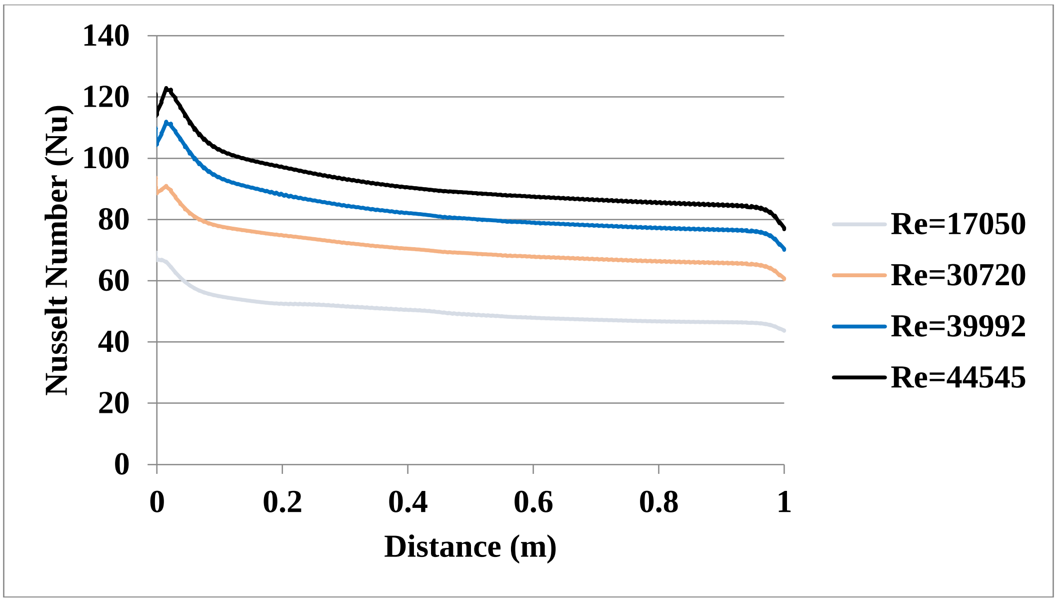

Nusselt Number (Nu)
140
120
100
80
60
40
20
0
0
0.2
0.4
0.6
0.8
1
Distance (m)
Re=17050
Re=30720
Re=39992
Re=44545